BIOCHEMISTRY
including biophysical chemistry & molecular biology

Article

pubs.acs.org/biochemistry

Restricting the ψ Torsion Angle Has Stereoelectronic Consequences on a Scissile Bond: An Electronic Structure Analysis

Eric R. Strieter* and Trisha L. Andrew

Department of Chemistry, University of Wisconsin—Madison, Madison, Wisconsin 53706, United States

Supporting Information

ABSTRACT: Protein motion is intimately linked to enzymatic catalysis, yet the stereoelectronic changes that accompany different conformational states of a substrate are poorly defined. Here we investigate the relationship between conformation and stereoelectronic effects of a scissile amide bond. Structural studies have revealed that the C-terminal glycine of ubiquitin and ubiquitin-like proteins adopts a *syn* ($\psi \sim 0°$) or *gauche* ($\psi \sim \pm 60°$) conformation upon interacting with deubiquitinases/ubiquitin-like proteases. We used hybrid density functional theory and natural bond orbital analysis to understand how the stereoelectronic effects of the scissile bond change as a function of φ and ψ torsion angles. This led to the discovery that when ψ is between 30° and −30° the scissile bond becomes geometrically and electronically deformed. Geometric distortion occurs through pyramidalization of the carbonyl carbon and amide nitrogen. Electronic distortion is manifested by a decrease in the strength of the donor−acceptor interaction between the amide nitrogen and antibonding orbital (π^*) of the carbonyl. Concomitant with the reduction in $n_N \rightarrow \pi^*$ delocalization energy, the sp^2 hybrid orbital of the carbonyl carbon becomes richer in p-character, suggesting the *syn* configuration causes the carbonyl carbon hybrid orbitals to adopt a geometry reminiscent of a tetrahedral-like intermediate. Our work reveals important insights into the role of substrate conformation in activating the reactive carbonyl of a scissile bond. These findings have implications for designing potent active site inhibitors based on the concept of transition state analogues.

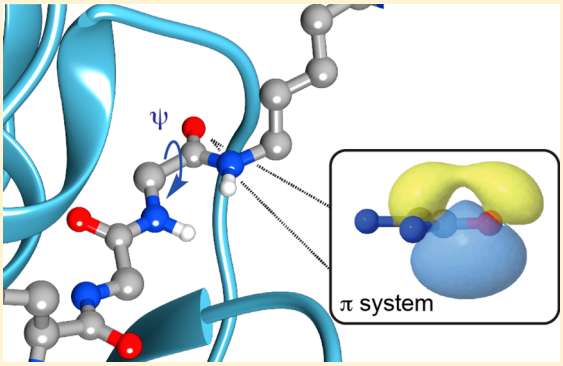

Stereoelectronic effects dictate structure and reactivity in organic chemistry.[1] The concept of stereoelectronic effects is rooted in the interactions between orbitals. According to frontier molecular orbital theory, chemical reactions require overlap between the highest occupied molecular orbitals (HOMOs) and the lowest unoccupied molecular orbitals (LUMOs) of the reactants. When orbitals are properly aligned, donor−acceptor interactions can occur, stabilizing conformations and transition states. Consider the case of chorismate mutase, an enzyme that catalyzes the key step in the skikimate pathway by converting chorismate to prephenate. The [3,3]-sigmatropic rearrangement of chorismate proceeds through a chairlike transition state in which orbitals are correctly aligned.[2,3] Gaining access to the chair conformer, however, requires energy as other conformers are more populated in solution. Chorismate mutase facilitates this process by rapidly converting the nonproductive states to the chair conformation.[4] This example illustrates that a structure resembling the transition state [also called a near attack conformer (NAC)] can be embedded within the Boltzmann distribution of ground state substrate conformations.[5] The key is for an enzyme to perturb the distribution in favor of the NAC.

Our lab has been interested in examining whether the concept of NACs applies to the isopeptidase activity of deubiquitinases (DUBs) and ubiquitin-like (Ubl) proteases. DUBs and Ubl proteases catalyze the removal of ubiquitin (Ub) and Ubl proteins from target proteins by hydrolytically cleaving the isopeptide bond between the Ub/Ubl C-terminal glycine and the ε-amino group of a substrate lysine[6,7] (Figure 1A). The general mechanism involves formation of a Michaelis complex with a Ub/Ubl−protein conjugate, nucleophilic attack of an active site thiolate on the C-terminal carbonyl carbon of Ub or a Ubl, generation of a thioester acyl−enzyme intermediate, and hydrolysis to liberate the free enzyme and Ub/Ubl (Figure 1B). Structural studies of Michaelis complexes have shown that the C-terminal glycine of Ub/Ubls (the P1 residue using the protease nomenclature) is confined to ψ angles that fluctuate between *syn* and *gauche* conformations ($-60° < \psi < 20°$)[8−13] (Figure 1C and Table 1). According to quantum mechanics/molecular mechanics simulations, the *syn* conformer rapidly isomerizes back to the *anti* configuration in the absence of a protease.[14] However, in the presence of an enzyme, the *syn* conformer is preferred because the vicinal NH groups of P1-Gly engage in a hydrogen bond network. The question is whether the *syn* configuration places the scissile carbonyl in a reactive conformation.

Received: April 16, 2015
Revised: August 31, 2015
Published: September 2, 2015

DOI: 10.1021/acs.biochem.5b00845
Biochemistry 2015, 54, 5748−5756

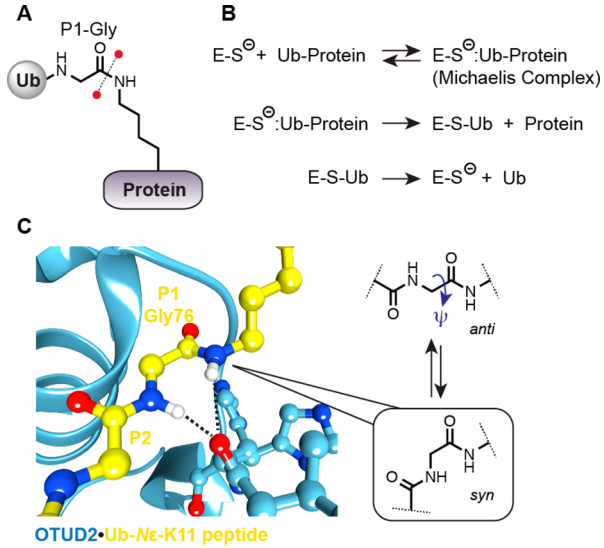

Figure 1. Cysteine-dependent DUBs/Ubl proteases cleave isopeptide bonds between the C-terminus of Ub/Ubls and the ε-amino groups of substrate lysine residues. (A) Structure of the isopeptide bond showing the scissile bond (dotted line with red circles). (B) Minimal mechanism of cysteine-dependent DUBs/Ubl proteases. (C) Close-up of a Michaelis complex between OTUD2 Cys160Ala and a Ub-*Nε*-K11 peptide (Protein Data Bank entry 4BOS).[11] A backbone carbonyl of OTUD2 (Ile266) forms a bifurcated hydrogen bond (dotted lines) with the *syn* confomer of the C-terminal glycine (Ub Gly76). The *anti*–*syn* interconversion is shown on the right.

We sought to address this problem by investigating the geometric and stereoelectronic changes that occur in P1-Gly as a function of conformation. The primary stereoelectronic effect that influences the reactivity of an amide bond is the donor–acceptor interaction between the nitrogen lone pair and the adjacent carbonyl antibonding orbital (herein termed the $n_N \rightarrow \pi^*$ interaction).[15] Unlike the chorismate example, the hypothesis is that activation of a scissile carbonyl requires a reduction in the level of orbital overlap by minimizing the $n_N \rightarrow \pi^*$ interaction.[15,16] Consistent with this idea, model compounds of twisted amides bearing an orthogonal nitrogen lone pair and carbonyl π^* orbital are 10^7–10^{11} times more susceptible to hydrolysis than planar amides.[17−19] How proteases contort an imidic bond and reduce resonance stabilization in an actual peptide substrate is, however, unclear. A few reports suggest the key to activation is rotation around the ω torsion angle in the form of *cis*–*trans* isomerization.[20,21] Other studies argue that scissile bond distortion depends on ψ, as imidic bond twisting and carbonyl pyramidalization occur over a range of ψ angles (i.e., when ψ is close to ±30°, ±90°, and ±150°).[22−26]

Because the ψ angle is confined for P1-Gly in Michaelis complexes of substrate-bound DUBs, we decided to focus on the relationship between the $n_N \rightarrow \pi^*$ interaction and ψ. Using hybrid density functional theory and natural bond orbital (NBO) analysis, we show that when P1-Gly of Ub/Ubl conjugates is forced to adopt a *syn* conformation ($-30° \leq \psi \leq 30°$) the carbonyl and amide nitrogen experience out-of-plane deformations and there is a corresponding decrease in the extent of $n_N \rightarrow \pi^*$ interaction. These geometric and electronic distortions are also accompanied by a reorganization of hybrid atomic orbitals. Our findings suggest that rotation around the ψ torsion angle can activate the scissile bond for cleavage.

COMPUTATIONAL METHODS

Model Used in Computational Studies. Through the action of three enzymes, E1–E3, the C-terminal glycine of Ub and Ubls is covalently tethered to the ε-amino group of substrate lysine residues to furnish an isopeptide bond.[27] We sought to mimic the isopeptide bond using the model tripeptide **I** (Figure 2), as it encompasses the C-terminal Gly-Gly motif of Ub/Ubls along with lysine. The glycine attached to the ε-amino group of Lys is the P1 site using the protease nomenclature developed by Schechter and Berger.[28]

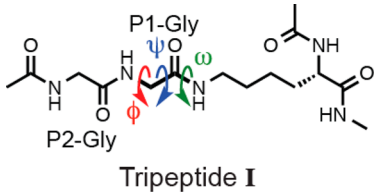

Figure 2. Structure of model tripeptide **I** showing the three torsion angles (φ, ψ, and ω) investigated in this study.

Geometry Optimization. Hybrid density functional theory as implemented in Gaussian '09[29] was employed to assess the conformational preferences of P1-Gly of tripeptide **I**. Full geometry optimizations were performed in water using a polarizable continuum model at the B3LYP/6-311++G(2d,p) level of theory.[30,31] The φ torsion angle was varied in 30° increments, and ψ was rotated in 10° increments, with subsequent energy minimization. The fractional population of

Table 1. Torsion Angles (φ and ψ) of P1 and P2 Glycines in the Presence and Absence of DUBs and Ubl Proteases[8,9,11−13,50−52]

Protein Data Bank	resolution (Å)	DUB/Ubl protease	Ub/Ubl conjugate	scissile bond	P1 φ (deg)	P1 ψ (deg)	P2 φ (deg)	P2 ψ (deg)
2IY0	2.8	SENP1	SUMO-1-RanGAP1	Gly(P2)-Gly(P1)-*Nε*-Lys	−134	−29	−163	143
2IO2	2.9	SENP2	SUMO-1-RanGAP1	Gly(P2)-Gly(P1)-*Nε*-Lys	−169	−22	−146	155
2IO3	3.2	SENP2	SUMO-2-RanGAP1	Gly(P2)-Gly(P1)-*Nε*-Lys	177	−8	−167	168
4BOS	2.3	OTUD2	Ub-*Nε*-K11 peptide	Gly(P2)-Gly(P1)-*Nε*-Lys	165	−16	−153	167
4KSL	2.8	OTULIN	Met1-linked Ub2	Gly(P2)-Gly(P1)-*Nα*-Met	136	7	94	137
3ZNZ	1.9	OTULIN	Met1-linked Ub2	Gly(P2)-Gly(P1)-*Nα*-Met	141	17	−113	136
3WXE	2.5	CYLD	Met1-linked Ub2	Gly(P2)-Gly(P1)-*Nα*-Met	169	−24	−163	180
3WXG	3.1	CYLD	K63-linked Ub2	Gly(P2)-Gly(P1)-*Nε*-Lys	147	−59	−156	−174
3UIP	2.3	none	SUMO-1-RanGAP1	Gly(P2)-Gly(P1)-*Nε*-Lys	−137	−155	−64	162
3UIO	2.6	none	SUMO-1-RanGAP1	Gly(P2)-Gly(P1)-*Nε*-Lys	−155	−162	−66	169
2W9N	2.2	none	Met1-linked Ub2	Gly(P2)-Gly(P1)-*Nα*-Met	−68	159	159	145

DOI: 10.1021/acs.biochem.5b00845
Biochemistry 2015, 54, 5748−5756

each conformer was calculated using the Boltzmann distribution equation and plotted as a function of φ and ψ. The data are presented in Table S1.

Out-of-Plane Deformations. The out-of-plane deformation of the imidic C(O)−N group in each conformer of tripeptide **I** can be described in terms of its internal orthogonal coordinates τ, χ_C, and χ_N.[32,33] The coordinate τ corresponds to the mean twisting angle around the C−N bond ranging from 0° (planar amide) to 90° (when the nitrogen lone pair is orthogonal to the carbonyl π^* system), and χ_C and χ_N represent the out-of-plane bending angles of the C and N atoms, respectively (Figure 3). In a planar sp^2 hybridized system

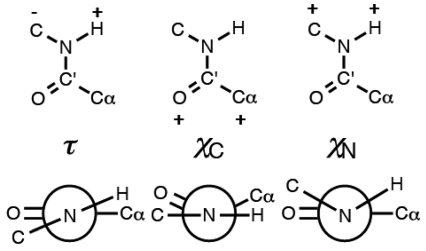

Figure 3. Internal coordinate system describing out-of-plane deformations around the scissile bond. Positive and negative signs indicate movement of atoms relative to neighboring groups.

χ_C and χ_N should be 0°. The geometrical meaning of τ, χ_C, and χ_N can be understood by defining the four torsion angles ω_1 = O−C′−N−C, ω_2 = Cα−C′−N−H, ω_3 = Cα−C′−N−C, and ω_4 = O−C′−N−H. Using these angles $\tau = (\omega_1 + \omega_2)/2$, $\chi_C = \omega_1 - \omega_3 + \pi \pmod{2\pi}$, and $\chi_N = \omega_2 - \omega_3 + \pi \pmod{2\pi}$. As a second measure of out-of-plane deformations, we calculated the sum of the bond angles around the P1 carbonyl group of tripeptide **I** as a function of φ, ψ angles. For a perfectly planar system the sum is 360° and it should decrease as the carbonyl deviates from planarity. The coordinates for each conformer are presented in Table S2.

Changes in Resonance Stabilization. NBO analysis was performed using NBO 6.0[34] interfaced into Gaussian '09. NBO analysis transforms the nonorthogonal atomic orbitals from the HF wave function into natural atomic orbitals (NAOs), natural hybrid orbitals (NHOs), and natural bond orbitals (NBOs). NBO transformations yield filled orbitals with high occupancies, which allow for the analysis of donor−acceptor interactions through second-order perturbation theory. The energy values from the second-order perturbation method provide a reasonable quantitative description of the magnitude of resonance stabilization through the $n_N \rightarrow \pi^*$ interaction.[35,36] NBO deletion analysis was also performed using the B3LYP/6-311++G(2d,p)-optimized structures. It is important to point out that the NBO method overestimates charge-transfer energies compared to the results of other localized wave function methods.[37] Nevertheless, the trends obtained from NBO calculations are the same as those produced by these other methods. More importantly, the overestimation of charge-transfer energies will be the same for each conformer in this study. NBO second-order perturbation data are presented in Table S3.

Hybrid Orbital Distortions. NBO transformations lead to NHOs, which represent optimal fits to electronic occupancies in terms of known angular properties of atomic orbitals. NHOs can therefore be used to measure percent p character and percent s character.[38] The hybridization data for each conformer are presented in Table S4.

RESULTS

The P1 Residue Is Conformationally Restricted in the Presence of DUBs and Ubl Proteases. Structures of catalytically inactive forms of cysteine-dependent DUBs and Ubl proteases bound to native substrates provide important insights into the geometrical changes that occur upon forming a Michaelis complex. To date, eight structures have been reported at resolutions between 1.9 and 3.2 Å (Table 1).[8−13] In all cases, the DUB or Ubl protease has been rendered inactive through a C-to-S or C-to-A substitution. Conformational analysis of the scissile bond reveals the ψ torsion angle of P1-Gly decreases upon formation of a Michaelis complex (Table 1; ψ moves from ±160° in the absence of a protease to between −60° and 20° in the presence of a protease). When $\psi \approx 0°$, the vicinal NH groups of P1-Gly are essentially eclipsing one another in a *syn* configuration (Figure 1C). For comparison, we also analyzed the conformation at the P2 site. These data demonstrate that upon engagement of a protease, conformational changes are largely limited to the P1 position, as the geometry at P2 remains relatively invariant (average P2 glycine ψ = 154°).

What restricts the conformation of P1-Gly is a backbone carbonyl of the protease. The cysteine protease DUBs and SENPs are characterized by the presence of a Cys-His-Asp/Asn catalytic triad.[39] According to available structures, the catalytic Cys is invariably positioned at the N-terminus of an α-helix, while the His and Asp/Asn residues are located within β-strands or loop regions. In all of the Michaelis complexes, there is a backbone carbonyl next to the catalytic His that is pointing toward the two NH groups of P1-Gly (Figure 1C). This carbonyl forms bifurcated hydrogen bonds, as measurements reveal hydrogen bonding criteria are satisfied in each structure; the donor−acceptor distances are 2.86 ± 0.16 and 3.06 ± 0.19 Å, the H···O distances 1.90 ± 0.19 and 2.19 ± 0.14 Å, and N−H···O bond angles are 160.0 ± 9.9° and 145.9 ± 15.0°.[40] Because the strength of bifurcated hydrogen bonds is estimated to be ∼2−3 kcal mol^{-1},[41] formation of such an interaction likely compensates for the allylic strain imposed by the *syn* configuration. We propose bifurcated hydrogen bonds are conserved in each Michaelis complex, as superposition aligns the active sites of all cysteine-dependent DUBs and Ubl proteases.

To understand how locking P1-Gly into a *syn* conformation could affect the energetics of the system, we constructed a Ramachandran surface of tripeptide **I**, a model for the isopeptide linkage (Figure 2). This was achieved by performing density functional theory (DFT) calculations at the B3LYP/6-311++G(2d,p) level. The φ torsion angle was varied in 30° increments, and ψ was rotated in 10° increments, with subsequent energy minimization. The fractional population of each conformer was then plotted as a function of φ and ψ (Figure 4A and Table S1). The resulting contour map is in accord with the canonical clustering of glycine conformations at ψ = 180° and ψ = 0°.[42,43] Placing the φ,ψ coordinates from each of the crystal structures on the Ramachandran plot indicates the *syn* and *gauche* conformations are in allowed space, with energies that are ∼1−3 kcal mol^{-1} higher than those of the *anti* configurations observed in the absence of a protease (Figure 4B).

DOI: 10.1021/acs.biochem.5b00845
Biochemistry 2015, 54, 5748−5756

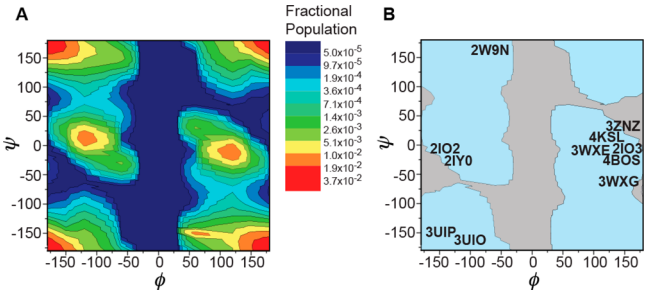

Figure 4. C-Terminal glycine of Ub/Ubls that adopts a *syn* conformation when bound to DUBs and Ubl proteases. (A) Ramachandran plot for P1-Gly of tripeptide **I**. Fractional populations were calculated using the Boltzmann distribution equation. Red corresponds to heavily populated conformers, while blue represents high-energy species. (B) Coordinates for P1-Gly of protease-bound and unbound Ub/Ubl conjugates are mapped on the Ramachandran plot for glycine. The allowed conformational space is colored blue, and the forbidden conformations are colored gray.

The Scissile Bond Is Distorted in Michaelis Complexes. With the identification of the *syn* conformer within the Boltzmann distribution of ground state conformations, we sought to determine whether the scissile bond is distorted in this configuration. Out-of-plane deformations of an amide bond can be described by the sum of bond angles as well as angles χ_C, χ_N, and τ (Table S2).[32,33]

We calculated the sum using three bond angles: Cα−C′−O, N−C′−O, and Cα−C′−N. Any deviation from trigonal planar geometry should lead to a sum of <360°. As evidenced by what ostensibly look like horizontal stripes in φ,ψ space, there are small (<0.3°) but significant (>2σ) deviations in trigonal planar geometry (Figure 5A). This indicates that the geometry of the carbonyl is dependent on the ψ torsion angle. The most significant distortions ($\Sigma \sim 5\sigma$) occur when glycine has φ,ψ coordinates of (60°,60°) and (140°,25°). On the left side of the map (φ < 0°), there is a smaller departure from trigonal planar geometry. However, there are points within this region where the sum is approximately 4σ, e.g., when the φ,ψ coordinates are (−140°,−25°) and (−60°,−60°).

A plot of χ_C as a function of φ and ψ reflects what we observe for the sum of the bond angles (Figure 5B). The largest χ_C values are 6° at (140°,25°) and −5° at (−140°,−25°), with a mean of 0.5°. Comparing these values to those obtained from crystal structures of serine proteases bound to proteinaceous inhibitors (χ_C between −10° and −20°) indicates a smaller degree of pyramidalization.[44] Nevertheless, χ_C values at the extremes strongly deviate from the mean, and it is at the extremes where the greatest overlap exists with the *syn* configuration of P1-Gly.

From the χ_C map, we can also extract information about the direction of pyramidalization. This is important as it relates to which prochiral face of an amide bond a nucleophile will add. A negative χ_C value predisposes the carbonyl carbon to *si* face addition. Conversely, a positive χ_C value means the carbonyl carbon is prone to *re* face attack. Focusing in on regions of the map occupied by the Michaelis complexes (Table 1 and Figure 4B), we find that in the lower left quadrant (−170° < φ <

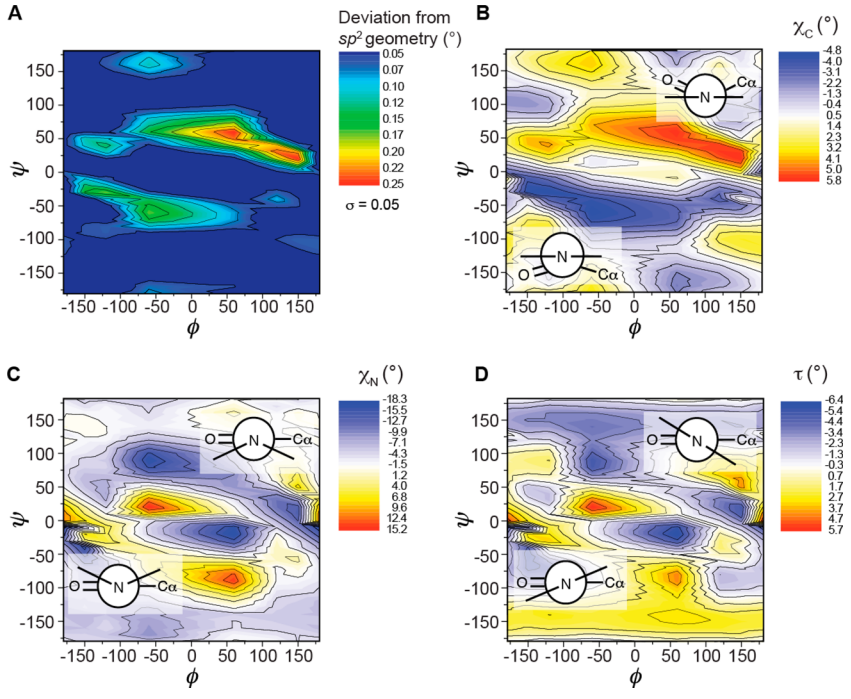

Figure 5. Conformational dependence of scissile bond distortion. (A) Contour map showing deviations from trigonal planar geometry as a function of φ and ψ torsion angles. The sum of bond angles Cα−C′−O, N−C′−O, and Cα−C′−N was calculated for each geometry-optimized structure of tripeptide **I**. The scale from blue to red represents the deviation from the idealized 360° geometry. The standard deviation (σ) for these changes is 0.05 (determined using φ = 180°, ±150°, ±120°, and ±60°). Distortions considered significant are >2σ (shown from green to red). (B) Contour map of χ_C as a function of φ and ψ torsion angles. Regions in blue (negative) and red (positive) represent the greatest deviations from planar (χ_C = 0) geometry. The mean χ_C value is 0.5 (determined using φ = 180°, ±150°, ±120°, and ±60°). (C) Contour map of χ_N as a function of φ and ψ torsion angles. Regions in blue (negative) and red (positive) represent the greatest deviations from planar (χ_N = 0) geometry. The mean χ_N value is −3.4 (determined using φ = 180°, ±150°, ±120°, and ±60°). (D) Contour map of τ as a function of φ and ψ torsion angles. Regions in blue (negative) and red (positive) represent the greatest twisting motion. The mean τ value is −0.4.

DOI: 10.1021/acs.biochem.5b00845
Biochemistry 2015, 54, 5748−5756

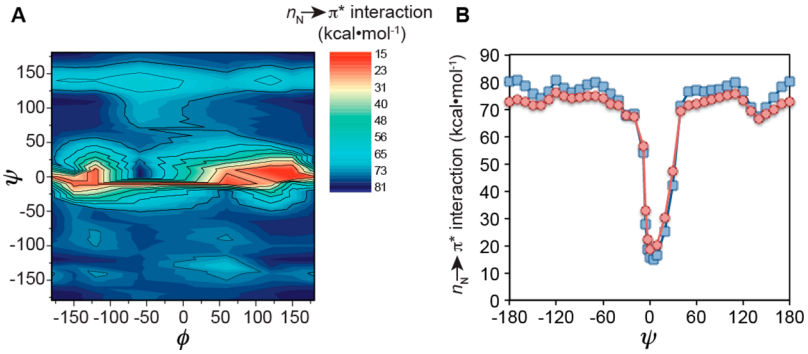

Figure 6. Delocalization energy is dependent on ψ. (A) Delocalization energy landscape of tripeptide **I**. Geometry-optimized structures of **I** were subjected to NBO analysis, and the donor−acceptor interaction was measured between the nitrogen lone pair of electrons (n_N) and the π^* system of the carbonyl. The colors indicate the magnitude of the $n_N \rightarrow \pi^*$ interaction, ranging from the global maximum (blue) to the global minimum (red). (B) Delocalization energy as a function of ψ using two methods: perturbation theory (blue squares) and quasi-variational theory (red circles). The φ torsion angle was fixed at 150° for these calculations.

−70°; −40° < ψ < 0°) the carbonyl pyramidalizes in the downward direction [χ_C is negative (see Figure 3)]. While in the upper right quadrant (70° < φ < 170°; 10° < ψ < 40°), the carbonyl pyramidalizes upward. Considering the orientation of P1-Gly in the active site of DUBs/Ubl proteases, the thiolate must add to the *si* face of the reactive carbonyl. This implies that the reactive conformation could be limited to −170° < φ < −70° and −40° < ψ < 0°.

According to the χ_N map (Figure 5C), the overall degree of pyramidalization is much larger than that for χ_C (values at the extremes are −18° and 15°). This indicates that the carbonyl carbon has a resistance to out-of-plane bending stronger than that of nitrogen. Another difference between χ_C and χ_N is that the out-of-plane deformations are more localized for the latter. For example, χ_C deformations essentially span a full rotation around φ when ψ falls between ±10° and ±40°, whereas with χ_N there are more distinct clusters. These results demonstrate that although χ_N has a dependence on φ greater than that of χ_C, there are still regions of significant overlap between the two angles.

The trends for τ are similar to those for χ_N (Figure 5D). A negative twist occurs with coordinates 110° < φ < 150° and 10° < ψ < 40°, and a positive twist manifests when −170° < φ < −70° and −40° < ψ < −10°. The difference between χ_N and τ is in their magnitude, as pyramidalization occurs to a much greater extent than twisting. Via combination of these results with those from the χ_C analysis, it evident that there are three scissile bond geometries represented by the Michealis complexes: one in which the scissile bond has ($+\tau$,$+\chi_N$,$-\chi_C$) coordinates, another in which the coordinates are ($-\tau$,$-\chi_N$, $+\chi_C$), and one in which the parameters do not significantly deviate from zero. From this structure correlation analysis, we conclude that the majority of crystallographically characterized Michaelis complexes depict a distorted scissile bond primed for nucleophilic addition.

Resonance Stabilization Is Dependent on Conformation. Nitrogen pyramidalization is accompanied by an $sp^2 \rightarrow sp^3$ rehybridization. During this transition, there is greater mixing of the nitrogen s and p atomic orbitals, which decreases the energy of the nitrogen lone pair (n_N). Because the magnitude of the donor−acceptor $n_N \rightarrow \pi^*$ interaction is inversely proportional to the difference in energy between n_N and the carbonyl π^* system, lowering the energy of the lone pair will lead to a decrease in the strength of the interaction. Nitrogen pyramidalization should therefore coincide with a decrease in the $n_N \rightarrow \pi^*$ interaction. To test this, we turned to NBO analysis as it transforms a quantum mechanical wave function into orbitals corresponding to Lewis structures with localized bonds and lone pairs.[45]

A delocalization energy landscape for P1-Gly of tripeptide **I** shows qked changes in the magntidue of the $n_N \rightarrow \pi^*$ interaction. When φ and ψ are 180°, the lone pair of the amide nitrogen is maximally delocalized into the π^* of the carbonyl (Figure 6A). The absolute value of resonance stabilization is overestimated by second-order perturbation measurements[37] (~80 kcal mol^{-1}) because it does not include the increase in the number of steric repulsions resulting from geometric changes associated with resonance delocalization. The empirical resonance energy corresponds approximately to the free energy of activation for rotation around the imidic C−N bond (reported to be 11−13 kcal mol^{-1} for glycine),[46] because resonance is completely lost in the transition state of this isomerization. Therefore, it is important to consider relative changes in NBO-derived stabilization energies, not the absolute energy values. Further inspection of the surface reveals two distinct regions where there is a significant decrease in the $n_N \rightarrow \pi^*$ interaction: one is on the left side when −180° < φ < −100°, and the other is on the right side when 40° < φ < 180° (Figure 6A). In both cases, the magnitude of the $n_N \rightarrow \pi^*$ interaction diminishes at ψ angles between 30° and −30°. A decrease in resonance stabilization is not observed for the adjacent P2 glycine (Table S3). As ψ diverges from 180°, the strong $n_N \rightarrow \pi^*$ interaction is replaced with a much weaker interaction between the nitrogen lone pair and the σ^* orbital of the C=O bond.

To reinforce the validity of these computational results, we also performed deletion analysis. Computational deletion of donor−acceptor interactions is based on quasi-variational theory instead of perturbation theory and provides a second measure of the $n_N \rightarrow \pi^*$ interaction.[38] The results of deletion analyses are in good agreement with those from second-order perturbation theory (Figure 6B). For instance, at ψ = 0°, quasi-variational theory estimates a 74% decrease in the extent of the $n_N \rightarrow \pi^*$ interaction relative to the median, and perturbation theory yields an 80% decrease. Our NBO results are therefore consistent with the prediction that nitrogen pyramidalization and loss of resonance stabilization overlap in several regions within the conformational landscape of glycine. More importantly, these results highlight the relationship between ψ and electronic changes to the scissile carbonyl.

DOI: 10.1021/acs.biochem.5b00845
Biochemistry 2015, 54, 5748−5756

The *syn* Conformation Distorts the Carbonyl Orbitals in the Scissile Bond. Next, we sought to investigate whether changes in electronic delocalization and carbonyl geometry are accompanied by a rehybridization of the carbonyl orbitals. Using the natural hybrid orbitals from NBO analyses, we measured the p character in interhybrid orbitals that comprise the σ framework of the carbonyl.[38] For an ideal sp^2-hybridized carbonyl carbon, the p character should be approximately 66%. Indeed, this is the case for most of the rotameric states of **I** when φ is maintained at 150° (Figure 7A). However, when ψ closes in on 0°, there is a sharp increase in p character, reaching ~83% when the vicinal NH groups are fully eclipsed. These results suggest the carbonyl rehybridizes from sp^2 to sp^3 as the glycine is forced into a *syn* configuration.

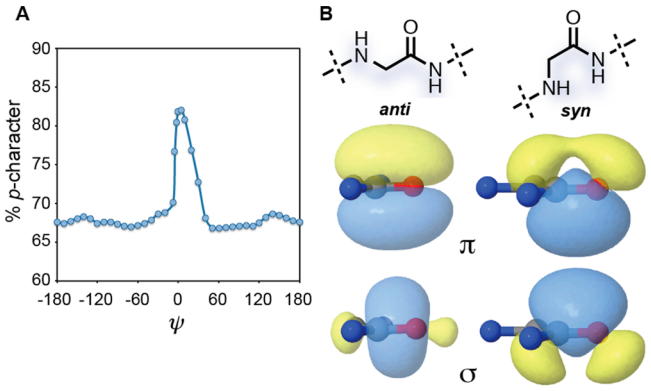

Figure 7. Carbonyl is distorted in the *syn* configuration. (A) Percent p character of the carbonyl hybrid orbital as a function of ψ when φ = 150°. (B) NBOs of the scissile carbonyl σ and π orbitals were constructed using the program Jmol (orbital cutoff of 0.02). Both the *anti* (ψ = 180°) and *syn* (ψ = 0°) configurations are shown. Atoms have been removed for the sake of clarity; carbons are colored gray, oxygens red, and nitrogens blue.

To understand how the carbonyl could undergo rehybridization yet retain an overall geometry resembling a trigonal carbon, we examined the localized NBOs of the σ and π systems. Comparing the NBOs of the *anti* and *syn* conformers reveals that in the latter the σ bond no longer lies along the C═O internuclear axis (Figure 7B). Instead, there is a tilt in the hybrid orbitals giving rise to a bonding orbital that is above the axis. The π system is almost the mirror image. Unlike a canonical π bond, the p orbitals are not at a 90° angle, as the axis of the carbon p orbital is again tilted by ~30° with respect to the C═O internuclear axis. This results in a rather unique bonding arrangement, with strong overlap between the lobes of the p orbitals that are tilted toward one another and relatively weak overlap with the lobes that are leaning away from each other. The antibonding π^* NBO shows a similar disposition of orbitals. Together, these results suggest that although the C═O bond remains intact in the *syn* configuration the orbitals resemble a sp^3-like geometry. This can have significant implications for reactivity, as the carbonyl does not have to undergo a complete rehybridization during attack by an active site thiolate.

DISCUSSION

In this study, we used a quantum mechanical approach to show that the conformational restriction imposed by DUBs has significant electronic and geometric consequences on the scissile bond. Structures of Michaelis-like complexes composed of cysteine-dependent DUBs/Ubl proteases and native substrates reveal a conserved bifurcated hydrogen bonding network between a backbone carbonyl of the enzyme and the vicinal NH groups of the C-terminal Ub/Ubl glycine residue. This forces glycine into a *syn* configuration where the vicinial NH groups are nearly eclipsing one another. Using structure correlation analysis, a method pioneered by Bürgi and Dunitz,[47] we show that the conformations of glycine in crystal structures of Michaelis complexes correspond to distorted geometries. The carbonyl carbon and the amide nitrogen experience out-of-plane deformations in the *syn* conformation. Consequently, the canonical amide resonance stabilization is attenuated, and the amount of p character in the carbonyl carbon hybrid orbitals is increased. Our work therefore establishes that P1-Gly of DUB substrates is geometrically and electronically distorted to the extent that the scissile carbonyl resembles a putative tetrahedral transition state for acyl−enzyme formation.

Our results shed light on how proteases twist the imidic bond and weaken the $n_N \rightarrow \pi^*$ interaction. Conformational analysis of tripeptide **I** shows a correlation between the $n_N \rightarrow \pi^*$ interaction and peptide planarity. Via examination of the allowed region of the Ramachandran plot for glycine in **I**, it is evident that the magnitude of the $n_N \rightarrow \pi^*$ interaction is at its lowest when ψ is between 30° and −30°. Similarly, there is significant deviation from planarity (as measured by both the degree of carbonyl and nitrogen pyramidalization) when ψ is between 40° and −40°. These results are entirely consistent with the model that holds that ψ modulates both electronic ($n_N \rightarrow \pi^*$ interaction) and geometric (χ_C) parameters.[23] From a stereoelectronic point of view, the importance of ψ could be a result of steric interactions. As ψ moves closer to 0°, the four-electron closed-shell repulsion between the filled orbitals of the vicinal NH groups could force the carbonyl and nitrogen to pyramidalize,[48] which in turn would lead to a reduction in the $n_N \rightarrow \pi^*$ interaction. Thus, when ψ is restricted to small angles, DUBs, and likely many other cysteine proteases, promote the loss of resonance stabilization and render the carbonyl more reactive.

We also observe a direct correlation between the loss of resonance stabilization and an increase in the percent p character of the carbonyl sp^2 orbital. This increase manifests from a distortion of both the σ and π bonds. With the former, there is a loss of bonding along the internuclear C═O axis, whereas with the latter, a plane of symmetry is lost between the orbitals on both faces of the C═O bond. The net effect is a bonding pattern reminiscent of an sp^3-like carbon that is induced by simply rotating around the ψ torsion angle. This partial rehybridization of the scissile carbonyl could also contribute to the free energy of activation associated with bond cleavage. A fundamental step in the cleavage of Ub/Ubl−protein conjugates by cysteine-dependent DUBs/Ubl proteases is nucleophilic addition by an active site thiolate into the π^* orbital of the substrate carbonyl. If the carbonyl is forced to adopt an sp^3-like geometry prior to thiolate addition, then less reorganizational energy is required for the formation of a tetrahedral species.

The conformational plasticity of glycine is likely critical to achieving a configuration conducive to nucleophilic attack. The steric constraints of amino acid side chains prevent non-glycyl residues from occupying φ,ψ space with positive φ values.[42,49] Without a side chain, glycine can then populate an amount of φ,ψ space much larger that of non-glycyl residues. In fact,

DOI: 10.1021/acs.biochem.5b00845
Biochemistry 2015, 54, 5748−5756

nearly the whole right side ($\varphi > 0°$) of the Ramachandran plot for glycine is allowed. We propose it is the right side of the Ramachandran plot that has the greatest functional consequences. Structure correlation analysis reveals that the scissile bond has coordinates of $(+\tau,+\chi_N,-\chi_C)$ or $(-\tau,-\chi_N,+\chi_C)$, depending on whether glycine occupies the left or right side of the Ramachandran plot, respectively. When χ_C is negative, the carbonyl of glycine is predisposed to *si* face addition (Figure 8). However, because τ and χ_N are positive when χ_C is negative,

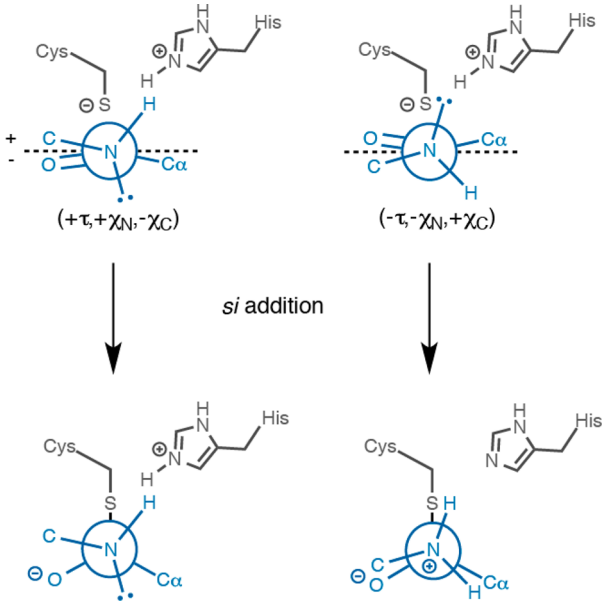

Figure 8. Schematic of *si* face addition of the active site thiolate to the carbonyl of P1-Gly.

the lone pair on nitrogen would be pointing in the opposite direction from the imidazolium species. Computational studies of cysteine proteases have shown that the transfer of a proton from the active site histidine is concerted with nucleophilic attack by the cysteine thiolate ion. When this is taken into account, an alternative scheme would involve *si* face addition to the carbonyl when it is pyramidalized upward ($+\chi_C$). This would place the nitrogen lone pair in the vicinity of the imidazolium ring and allow for protonation to occur simultaneously with nucleophilic attack. We favor this model for the following reasons. First, the degree of carbonyl pyramidalization is quite small and is probably less important in activating the carbonyl than nitrogen pyramidalization. Second, the largest window in which geometric and electronic distortions occur is on the right side of the Ramachandran plot.

Our findings have led to a molecular model for how DUBs/Ubl proteases activate their substrates for cleavage. We propose these enzymes twist P1-Gly into a *syn* configuration, destabilizing and distorting the scissile carbonyl. Flexibility in both the Ub/Ubl core as well as the C-terminus is likely to play a role in promoting an environment that perturbs the scissile carbonyl and ultimately drives catalysis. Our results have implications for not only our fundamental understanding of DUBs and Ubl proteases but also the design of transition state analogues that could bind with high affinity to the active sites of these enzymes. By mimicking a tetrahedral intermediate with a vicinal NH group in an eclipsing conformation, future studies will aim to develop molecules that act as tight-binding inhibitors.

■ ASSOCIATED CONTENT

Supporting Information

The Supporting Information is available free of charge on the ACS Publications website at DOI: 10.1021/acs.biochem.5b00845.

Table S1 (XLSX)
Table S2 (XLSX)
Table S3 (XLSX)
Table S4 (XLSX)

■ AUTHOR INFORMATION

Corresponding Author

*E-mail: strieter@chem.wisc.edu.

Funding

Financial support was provided by the University of Wisconsin—Madison and a National Institutes of Health grant (1RO1GM110543) to E.R.S.

Notes

The authors declare no competing financial interest.

■ ACKNOWLEDGMENTS

We thank Prof. Clark R. Landis for many helpful discussions.

■ REFERENCES

(1) Gorenstein, D. G. (1987) Stereoelectronic Effects in Biomolecules. *Chem. Rev. 87*, 1047−1077.
(2) Copley, S. D., and Knowles, J. R. (1985) The uncatalyzed Claisen rearrangement of chorismate to prephenate prefers a transition state of chair-like geometry. *J. Am. Chem. Soc. 107*, 5306−5308.
(3) Sogo, S. G., Widlanski, T. S., Hoare, J. H., Grimshaw, C. E., Berchtold, G. A., and Knowles, J. R. (1984) Stereochemistry of the rearrangement of chorismate to prephenate: chorismate mutase involves a chair transition state. *J. Am. Chem. Soc. 106*, 2701−2703.
(4) Guo, H., Cui, Q., Lipscomb, W. N., and Karplus, M. (2001) Substrate conformational transitions in the active site of chorismate mutase: their role in the catalytic mechanism. *Proc. Natl. Acad. Sci. U. S. A. 98*, 9032−9037.
(5) Bruice, T. C., and Lightstone, F. C. (1999) Ground State and Transition State Contributions to the Rates of Intramolecular and Enzymatic Reactions. *Acc. Chem. Res. 32*, 127−136.
(6) Clague, M. J., Barsukov, I., Coulson, J. M., Liu, H., Rigden, D. J., and Urbe, S. (2013) Deubiquitylases from genes to organism. *Physiol. Rev. 93*, 1289−1315.
(7) Komander, D., Clague, M. J., and Urbe, S. (2009) Breaking the chains: structure and function of the deubiquitinases. *Nat. Rev. Mol. Cell Biol. 10*, 550−563.
(8) Shen, L., Tatham, M. H., Dong, C., Zagorska, A., Naismith, J. H., and Hay, R. T. (2006) SUMO protease SENP1 induces isomerization of the scissile peptide bond. *Nat. Struct. Mol. Biol. 13*, 1069−1077.
(9) Reverter, D., and Lima, C. D. (2006) Structural basis for SENP2 protease interactions with SUMO precursors and conjugated substrates. *Nat. Struct. Mol. Biol. 13*, 1060−1068.
(10) Huang, D. T., and Schulman, B. A. (2006) Breaking up with a kinky SUMO. *Nat. Struct. Mol. Biol. 13*, 1045−1047.
(11) Mevissen, T. E., Hospenthal, M. K., Geurink, P. P., Elliott, P. R., Akutsu, M., Arnaudo, N., Ekkebus, R., Kulathu, Y., Wauer, T., El Oualid, F., Freund, S. M., Ovaa, H., and Komander, D. (2013) OTU deubiquitinases reveal mechanisms of linkage specificity and enable ubiquitin chain restriction analysis. *Cell 154*, 169−184.
(12) Keusekotten, K., Elliott, P. R., Glockner, L., Fiil, B. K., Damgaard, R. B., Kulathu, Y., Wauer, T., Hospenthal, M. K., Gyrd-Hansen, M., Krappmann, D., Hofmann, K., and Komander, D. (2013) OTULIN antagonizes LUBAC signaling by specifically hydrolyzing Met1-linked polyubiquitin. *Cell 153*, 1312−1326.

DOI: 10.1021/acs.biochem.5b00845
Biochemistry 2015, 54, 5748−5756

(13) Sato, Y., Goto, E., Shibata, Y., Kubota, Y., Yamagata, A., Goto-Ito, S., Kubota, K., Inoue, J., Takekawa, M., Tokunaga, F., and Fukai, S. (2015) Structures of CYLD USP with Met1- or Lys63-linked diubiquitin reveal mechanisms for dual specificity. *Nat. Struct. Mol. Biol. 22*, 222−229.
(14) Shi, T., Han, Y., Li, W., Zhao, Y., Liu, Y., Huang, Z., Lu, S., and Zhang, J. (2013) Exploring the desumoylation process of SENP1: a study combined MD simulations with QM/MM calculations on SENP1-SUMO1-RanGAP1. *J. Chem. Inf. Model. 53*, 2360−2368.
(15) Jencks, W. P. (1987) *Catalysis in chemistry and enzymology*, Dover, New York.
(16) Mock, W. L. (1975) Torsional strain considerations in the mechanism of the proteolytic enzymes, with particular application to carboxypeptidase A. *Bioorg. Chem. 4*, 270−278.
(17) Wang, Q. P., Bennet, A. J., Brown, R. S., and Santarsiero, B. D. (1991) Distorted Amides as Models for Activated Peptide N-C(O) Units 0.3. Synthesis, Hydrolytic Profile, and Molecular-Structure of 2,3,4,5-Tetrahydro-2-Oxo-1,5-Propanobenzazepine. *J. Am. Chem. Soc. 113*, 5757−5765.
(18) Lopez, X., Mujika, J. I., Blackburn, G. M., and Karplus, M. (2003) Alkaline hydrolysis of amide bonds: Effect of bond twist and nitrogen pyramidalization. *J. Phys. Chem. A 107*, 2304−2315.
(19) Mujika, J. I., Mercero, J. M., and Lopez, X. (2005) Water-promoted hydrolysis of a highly twisted amide: Rate acceleration caused by the twist of the amide bond. *J. Am. Chem. Soc. 127*, 4445−4453.
(20) Liu, B., Schofield, C. J., and Wilmouth, R. C. (2006) Structural analyses on intermediates in serine protease catalysis. *J. Biol. Chem. 281*, 24024−24035.
(21) Klabunde, T., Sharma, S., Telenti, A., Jacobs, W. R., Jr., and Sacchettini, J. C. (1998) Crystal structure of GyrA intein from Mycobacterium xenopi reveals structural basis of protein splicing. *Nat. Struct. Biol. 5*, 31−36.
(22) MacArthur, M. W., and Thornton, J. M. (1996) Deviations from planarity of the peptide bond in peptides and proteins. *J. Mol. Biol. 264*, 1180−1195.
(23) Improta, R., Vitagliano, L., and Esposito, L. (2011) Peptide bond distortions from planarity: new insights from quantum mechanical calculations and peptide/protein crystal structures. *PLoS One 6*, e24533.
(24) Esposito, L., De Simone, A., Zagari, A., and Vitagliano, L. (2005) Correlation between omega and psi dihedral angles in protein structures. *J. Mol. Biol. 347*, 483−487.
(25) Esposito, L., Vitagliano, L., Zagari, A., and Mazzarella, L. (2000) Pyramidalization of backbone carbonyl carbon atoms in proteins. *Protein Sci. 9*, 2038−2042.
(26) Berkholz, D. S., Driggers, C. M., Shapovalov, M. V., Dunbrack, R. L., Jr., and Karplus, P. A. (2012) Nonplanar peptide bonds in proteins are common and conserved but not biased toward active sites. *Proc. Natl. Acad. Sci. U. S. A. 109*, 449−453.
(27) Hershko, A., and Ciechanover, A. (1998) The ubiquitin system. *Annu. Rev. Biochem. 67*, 425−479.
(28) Schechter, I., and Berger, A. (1967) On the size of the active site in proteases. I. Papain. *Biochem. Biophys. Res. Commun. 27*, 157−162.
(29) Frisch, M. J., Trucks, G. W., Schlegel, H. B., Scuseria, G. E., Robb, M. A., Cheeseman, J. R., Scalmani, G., Barone, V., Mennucci, B., Petersson, G. A., Nakatsuji, H., Caricato, M., Li, X., Hratchian, H. P., Izmaylov, A. F., Bloino, J., Zheng, G., Sonnenberg, J. L., Hada, M., Ehara, M., Toyota, K., Fukuda, R., Hasegawa, J., Ishida, M., Nakajima, T., Honda, Y., Kitao, O., Nakai, H., Vreven, T., Montgomery, J. A., Jr., Peralta, J. E., Ogliaro, F., Bearpark, M., Heyd, J. J., Brothers, E., Kudin, K. N., Staroverov, V. N., Kobayashi, R., Normand, J., Raghavachari, K., Rendell, A., Burant, J. C., Iyengar, S. S., Tomasi, J., Cossi, M., Rega, N., Millam, J. M., Klene, M., Knox, J. E., Cross, J. B., Bakken, V., Adamo, C., Jaramillo, J., Gomperts, R., Stratmann, R. E., Yazyev, O., Austin, A. J., Cammi, R., Pomelli, C., Ochterski, J. W., Martin, R. L., Morokuma, K., Zakrzewski, V. G., Voth, G. A., Salvador, P., Dannenberg, J. J., Dapprich, S., Daniels, A. D., Farkas, Ö., Foresman, J. B., Ortiz, J. V., Cioslowski, J., and Fox, D. J. (2009) *Gaussian '09*, revision D.01, Gaussian, Inc., Wallingford, CT.
(30) Becke, A. D. (1993) Density-functional thermochemistry. III. The role of exact exchange. *J. Chem. Phys. 98*, 5648−5652.
(31) Lee, C., Yang, W., and Parr, R. G. (1988) Development of the Colle-Salvetti correlation-energy formula into a functional of the electron density. *Phys. Rev. B: Condens. Matter Mater. Phys. 37*, 785−789.
(32) Winkler, F. K., and Dunitz, J. D. (1971) The non-planar amide group. *J. Mol. Biol. 59*, 169−182.
(33) Gilli, G., Bertolasi, V., Bellucci, F., and Ferretti, V. (1986) Stereochemistry of the R1(X:)C(sp2)-N(sp3)R2R3 fragment. Mapping of the cis-trans isomerization path by rotation around the carbon-nitrogen bond from crystallographic structural data. *J. Am. Chem. Soc. 108*, 2420−2424.
(34) Glendening, E. D., and Weinhold, F. (2013) *Natural Bond Orbital 6.0*, University of Wisconsin—Madison, Madison, WI.
(35) Alabugin, I. V., and Zeidan, T. A. (2002) Stereoelectronic effects and general trends in hyperconjugative acceptor ability of sigma bonds. *J. Am. Chem. Soc. 124*, 3175−3185.
(36) Ruben, E. A., Plumley, J. A., Chapman, M. S., and Evanseck, J. D. (2008) Anomeric effect in "high energy" phosphate bonds. Selective destabilization of the scissile bond and modulation of the exothermicity of hydrolysis. *J. Am. Chem. Soc. 130*, 3349−3358.
(37) Kitaura, K., and Morokuma, K. (1976) A New Energy Decomposition Scheme for Molecular Interactions within the Hartree-Fock Approximation. *Int. J. Quantum Chem. 10*, 325−340.
(38) Weinhold, F., and Landis, C. R. (2012) *Discovering chemistry with natural bond orbitals*, Wiley, Hoboken, NJ.
(39) Storer, A. C., and Menard, R. (1994) Catalytic mechanism in papain family of cysteine peptidases. *Methods Enzymol. 244*, 486−500.
(40) McDonald, I. K., and Thornton, J. M. (1994) Satisfying hydrogen bonding potential in proteins. *J. Mol. Biol. 238*, 777−793.
(41) Feldblum, E. S., and Arkin, I. T. (2014) Strength of a bifurcated H bond. *Proc. Natl. Acad. Sci. U. S. A. 111*, 4085−4090.
(42) Ramachandran, G. N., Ramakrishnan, C., and Sasisekharan, V. (1963) Stereochemistry of polypeptide chain configurations. *J. Mol. Biol. 7*, 95−99.
(43) Head-Gordon, T., Head-Gordon, M., Frisch, M. J., Brooks, C. L., and Pople, J. A. (1991) Theoretical study of blocked glycine and alanine peptide analogs. *J. Am. Chem. Soc. 113*, 5989−5997.
(44) Marquart, M., Walter, J., Deisenhofer, J., Bode, W., and Huber, R. (1983) The Geometry of the Reactive Site and of the Peptide Groups in Trypsin, Trypsinogen and Its Complexes with Inhibitors. *Acta Crystallogr., Sect. B: Struct. Sci. 39*, 480−490.
(45) Weinhold, F., and Landis, C. R. (2005) *Valency and bonding: A natural bond orbital donor-acceptor perspective*, Cambridge University Press, Cambridge, U.K.
(46) Li, P., Chen, X. G., Shulin, E., and Asher, S. A. (1997) UV resonance Raman ground and excited state studies of amide and peptide isomerization dynamics. *J. Am. Chem. Soc. 119*, 1116−1120.
(47) Bürgi, H., and Dunitz, J. (1983) From crystal statics to chemical dynamics. *Acc. Chem. Res. 16*, 153−161.
(48) Rondan, N. G., Paddonrow, M. N., Caramella, P., and Houk, K. N. (1981) Nonplanar Alkenes and Carbonyls - a Molecular Distortion Which Parallels Addition Stereoselectivity. *J. Am. Chem. Soc. 103*, 2436−2438.
(49) Ramakrishnan, C., and Ramachandran, G. N. (1965) Stereochemical criteria for polypeptide and protein chain conformations. II. Allowed conformations for a pair of peptide units. *Biophys. J. 5*, 909−933.
(50) Rivkin, E., Almeida, S. M., Ceccarelli, D. F., Juang, Y. C., MacLean, T. A., Srikumar, T., Huang, H., Dunham, W. H., Fukumura, R., Xie, G., Gondo, Y., Raught, B., Gingras, A. C., Sicheri, F., and Cordes, S. P. (2013) The linear ubiquitin-specific deubiquitinase gumby regulates angiogenesis. *Nature 498*, 318−324.
(51) Gareau, J. R., Reverter, D., and Lima, C. D. (2012) Determinants of small ubiquitin-like modifier 1 (SUMO1) protein

DOI: 10.1021/acs.biochem.5b00845
Biochemistry 2015, 54, 5748−5756

specificity, E3 ligase, and SUMO-RanGAP1 binding activities of nucleoporin RanBP2. *J. Biol. Chem. 287*, 4740−4751.
(52) Komander, D., Reyes-Turcu, F., Licchesi, J. D., Odenwaelder, P., Wilkinson, K. D., and Barford, D. (2009) Molecular discrimination of structurally equivalent Lys 63-linked and linear polyubiquitin chains. *EMBO Rep. 10*, 466−473.

DOI: 10.1021/acs.biochem.5b00845
Biochemistry 2015, 54, 5748−5756